# 行政院國家科學委員會專題研究計畫 成果報告

## 新穎接枝型起孔洞劑之多孔性低介電材料探討(I)
## 研究成果報告(精簡版)

計 畫 類 別 ：個別型
計 畫 編 號 ：NSC 99-2221-E-009-177-
執 行 期 間 ：99 年 08 月 01 日至 100 年 07 月 31 日
執 行 單 位 ：國立交通大學材料科學與工程學系（所）

計 畫 主 持 人：呂志鵬

計畫參與人員：博士班研究生-兼任助理人員：邱詩雅
博士班研究生-兼任助理人員：涂弘恩

報 告 附 件 ：出席國際會議研究心得報告及發表論文

公 開 資 訊 ：本計畫涉及專利或其他智慧財產權，1 年後可公開查詢

中 華 民 國 100 年 10 月 31 日

中文摘要：　本計畫成功利用原子轉移自由基聚合反應合成出一種全新的反應性起孔洞劑：三氧乙基聚苯乙烯矽氧烷（triethoxy(polystyrene)silane, TEPSS）。並利用其本身的熱穩定性作為高溫起孔洞劑，成功將其應用於起孔洞劑延後移除積體製程（late-porogen removal integration scheme）中。隨後，更成功將 TEPSS 接枝（graft）於聚甲基矽氧烷（poly(methylsilsesquioxane), MSQ）母材上，避免起孔洞劑與母材之間相分離的情形，並且將起孔洞劑聚集的情況降至最低。

本研究報告中，將討論反應起始劑的濃度與溶劑對 TEPSS 分子量的影響，對於接枝後的低介電薄膜的化學結構、孔隙率和介電材數也將有所著墨。根據我們的實驗結果，發現使用和 TEPSS 擁有最接近溶解度參數的溶劑對二甲苯（p-xylene）和反應起始劑，會大幅降低 TEPSS 合成後的分子量。最後，由於反應性起孔洞劑的接枝反應與其擁有的低 PDI 值，最後的多孔性低介電 MSQ 薄膜擁有大小均勻的 18 奈米孔洞，孔隙率達到 31%且介電常數降至 2.37。

英文摘要：　We have developed mesoporous organosilicate films with high-temperature porogen suitable for a late-porogen removal integration scheme. A reactive porogen, triethoxy(polystyrene)silane (TEPSS) was synthesized via atom transfer radical polymerization (ATRP). TEPSS was then grafted onto poly(methylsilsesquioxane) (MSQ) matrix to circumvent the phase separation between matrix and porogen in the hybrid approach and minimize porogen aggregation.

The effects of concentration of initiator and reaction solvents on the molecular weight of TEPSS were also investigated. In this report, p-xylene which has the closest solubility parameter with initiator induced most reaction and decreased the TEPSS molecular weight largely. The chemical structure, porosity, dielectric of grafted-low-k film was investigated in this study. Our results shows porous low-k MSQ films possess uniform pore size, 18 nm for porosity 31%, primarily due to low PDI and reactive porogen, and the dielectric constant is decreased to 2.37.

行政院國家科學委員會補助專題研究計畫 ■ 成 果 報 告
□期中進度報告

# 新穎接枝型起孔洞劑之多孔性低介電材料探討

Novel porous low-k materials with grafted porogens: their synthesis, pore morphology and properties

計畫類別：■個別型計畫　□整合型計畫
計畫編號：NSC 99－2221－E－009－177－
執行期間：2010 年 08 月 01 日至 2011 年 07 月 31 日

執行機構及系所：國立交通大學材料科學與工程學系(所)

計畫主持人：呂志鵬
共同主持人：
計畫參與人員：邱詩雅、涂弘恩

成果報告類型(依經費核定清單規定繳交)：■精簡報告　□完整報告

本計畫除繳交成果報告外，另須繳交以下出國心得報告：
□赴國外出差或研習心得報告
□赴大陸地區出差或研習心得報告
■出席國際學術會議心得報告
□國際合作研究計畫國外研究報告

處理方式：除列管計畫及下列情形者外，得立即公開查詢
□涉及專利或其他智慧財產權，□一年□二年後可公開查詢

中　華　民　國 100 年 10 月　日

**中文摘要**

本計畫成功利用原子轉移自由基聚合反應合成出一種全新的反應性起孔洞劑：三氧乙基聚苯乙烯矽氧烷（triethoxy(polystyrene)silane, TEPSS）。並利用其本身的熱穩定性作為高溫起孔洞劑，成功將其應用於起孔洞劑延後移除積體製程（late-porogen removal integration scheme）中。隨後，更成功將 TEPSS 接枝（graft）於聚甲基矽氧烷（poly(methylsilsesquioxane), MSQ）母材上，避免起孔洞劑與母材之間相分離的情形，並且將起孔洞劑聚集的情況降至最低。

本研究報告中，將討論反應起始劑的濃度與溶劑對 TEPSS 分子量的影響，對於接枝後的低介電薄膜的化學結構、孔隙率和介電材數也將有所著墨。根據我們的實驗結果，發現使用和 TEPSS 擁有最接近溶解度參數的溶劑對二甲苯（p-xylene）和反應起始劑，會大幅降低 TEPSS 合成後的分子量。最後，由於反應性起孔洞劑的接枝反應與其擁有的低 PDI 值，最後的多孔性低介電 MSQ 薄膜擁有大小均勻的 18 奈米孔洞，孔隙率達到 31%且介電常數降至 2.37。

**關鍵字：低介電材料；反應性起孔洞劑；接枝反應；原子轉移自由基聚合反應**

**英文摘要**

We have developed mesoporous organosilicate films with high-temperature porogen suitable for a late-porogen removal integration scheme. A reactive porogen, triethoxy(polystyrene)silane (TEPSS) was synthesized via atom transfer radical polymerization (ATRP). TEPSS was then grafted onto poly(methylsilsesquioxane) (MSQ) matrix to circumvent the phase separation between matrix and porogen in the hybrid approach and minimize porogen aggregation.

The effects of concentration of initiator and reaction solvents on the molecular weight of TEPSS were also investigated. In this report, *p*-xylene which has the closest solubility parameter with initiator induced most reaction and decreased the TEPSS molecular weight largely. The chemical structure, porosity, dielectric of grafted-low-k film was investigated in this study. Our results shows porous low-k MSQ films possess uniform pore size, 18 nm for porosity 31%, primarily due to low PDI and reactive porogen, and the dielectric constant is decreased to 2.37.

**Keywords: low-k materials; porogen; grafting reaction; atom transfer radical polymerization (ATRP)**

**報告內容：**

**前言**

As the device scaling continues, the increase of propagation (RC) delay, crosstalk noise and power dissipation of the interconnect structure become limiting factors for ultra-large-scale integration of integrated circuits.[1,2] To minimize the RC delay increase, the industry introduces copper metallization, led by International Business Machine Corp. (IBM) in 1997, to reduce the resistance as well as improve electromigration performance of the wiring.[3] To further reduce the delay, low dielectric constant materials (low-*k*) materials[4] such as carbondoped oxide or SiLK™ (*k*=2.6-3.0)[5] are introduced starting 2001 to reduce the parasitic capacitance, which is 28-37% reduction from $SiO_2$ ($k_{TEOS}$=4.2) or 19-28% from fluorosilicate glass ($k_{FSG}$=3.7).[6,7] For ultra-low k materials (*k*<2.5) in 32 nm node and beyond, pores at various porosity have been incorporated into the dielectric matrix to reduce *k*-value. Most of ultra low-*k* films were prepared by introducing templating agent[8] into silica structure using spin-on solution coating or plasma-enhanced chemical vapor deposition.[9] The templating agent or pore generator (porogen) was then removed during the deposition or subsequent thermal process. However, due to large pore size/distribution or interconnected pores, porous low-*k* films faced some critical issues such as (1) low mechanical strength leading to delamination or cracks after chemical-mechanical polish (CMP) or packaging and (2) poor barrier/dielectric reliability due to non-continuous side-wall coverage of barrier. As a result, a late-porogen removal scheme, which uses a high-temperature porogen and new integration process to defer the formation of porous dielectric (*i.e.* the removal of high-temperature porogen after a metal/low-*k* layer is completed), was introduced to circumvent these issues.[10]

The common method for preparing porous low-*k* films is to mix porogen into a matrix such as spin-on glass in a solution, then spin-coat the matrix/porogen solution onto a substrate. For as-deposited scheme, low-temperature porogen will be removed immediately after deposition and cure step. For high-temperature porogen in late-porogen removal scheme, a cure step preferably at ≤300 °C is employed to form a crosslinked dielectric as the starting interlayer dielectric (ILD). High-temperature porogen is then burned out at 300-400 °C after CMP step in copper dual damascene process. However, there are serious reliability concerns such as interconnected pores and/or poor size distribution[11] due to enhanced diffusion and porogen aggregation during the cure step.[12,13] Such pore morphology leads to weak mechanical strength and insufficient barrier coverage at trench side-wall rendering it less suitable for applications in the copper/low-*k* backend interconnect. However, there is still room for improvement in terms of the pore size and especially the distribution for ultra low-*k* materials with high porosity (*P* > 40-50%).

**研究目的**

In order to circumvent the issues of large pore sizes, interconnected pores, and poor distribution in a matrix/porogen hybrid system caused by severe aggregation of porogen during the cure process, this proposal took a novel approach by grafting a functionalized porogen onto the backbone of low-*k* precursor, which is further crosslinked into a low-*k* matrix with well dispersed and discrete porogen to achieve excellent control of pore size and pore distribution. Therefore, we plan to synthesize the novel porogen with siloxane end-cap by atom transfer radical polymerization (ATRP).[14] ATRP involves an organic halide undergoing a reversible redox process catalyzed by a transition metal compound such as cuprous halide. The reactivity of ATRP reactivity is determined by monomer, metal catalyst, organic halides, temperature, and solvents. A number of

different types of copolymers can be prepared by ATRP such as random, block, and graft copolymers.[15] Also, polymer molecular weight and polydispersity index are controllable in ATRP, and final polymer structures with special functional groups are dictated by the structure of initiator. Then, this novel functionalized porogen is grafted onto the backbone of low-*k* precursor, which is further crosslinked to low-*k* matrix with well-dispersed and discrete porogens.

In particular, triethoxy(polystyrene)silane (TEPSS), in which polystyrene (PS) is one kind of high-temperature porogens, has been synthesized by ATRP reaction to achieve extremely low polydispersity, desirable for tight pore distribution. Subsequently, TEPSS will be grafted onto poly(methylsilsesquioxane) (MSQ) matrix to form a novel low-*k* MSQ material with grafting PS porogen, designated as TEPSS-MSQ. The advantages of TEPSS-MSQ over MSQ/PS hybrid on the pore morphology (pore size and distribution) will be quantitative illustrated by using SEM and GISAXS characterization.[16] Upon the confirmation of our proposed grafting porogen scheme, we investigated the effect of molecular weights of PS on the final pore size/distribution by adjusting the initiator contents and reaction time during ATRP step. Moreover, the impact of solvent compatibility on the final pore size and distribution will also be discussed in this report.

**文獻探討**

For the application of ultra low-*k* dielectrics (k≤2.5) as ILD for 32 nm node and beyond, large porosity was introduced into low-k materials matrix using porogens which is burned out immediately after dielectrics deposition[17] or after completion of a Cu/low-*k* metallization layer in the late-porogen removal scheme.[18] The common method for preparing porous low-*k* films is to mix porogen into a matrix, and then spin-coat the matrix/porogen solution onto a substrate. For spin-on dielectrics with large porosity, the pore size is relatively large with wide distribution compared to the porous dielectric deposited by PECVD method using small molecules as porogen. Such interconnect pores may be caused from the aggregation of porogen in the solution at room temperature, and even in the curing duration.[19] Large pore size and interconnected pores may detrimentally degrade the mechanical strength of ultra low-*k* film[20] such that it cannot meet the minimum requirements (~4 GPa) for applications in the copper/low-*k* backend interconnect.[21] However, for a mechanically robust low-*k* material and better reliability at trench side-wall, it is highly desirable to have small and well-dispersed pore sizes with tight distribution in the low-*k* films.[22,23] Approaches such as fast heating rate in the cure step or addition of surfactants had been undertaken to retard the porogen segregation in the solution and casted film to improve the pore size and distribution in porous low-*k* materials with limited success.[24] However, some issues were occurred in the heating process such as porogen aggregation and broad pore size distribution. To overcome those problems, Nguyen et al. reported the nanoporous MSQ films which prepared via star-shaped poly(ε-caprolactone) porogen in MSQ/PCL hybrids.[25] Pore sizes of nanoporous MSQ films were smaller than 20 nm in size. Further, Moonhor Ree group published the idea of "reactive porogen" by using six-armed poly( ε -caprolactone) (mPCL6) and MSQ as porogen and matrix, respectively.[26,27] The multi-arm (4-arm or 6-arm) poly(ε-caprolactone) where the arms were grown via atom transfer radical polymerization (ATRP) or block copolymers prepared by using consecutive ring-opening polymerization (ROP) and ATRP processed.[28,29] Pore sizes of porous low-*k* films which used mPCL6 as porogen was calculated around 5 nm with 40% porogen loading.[30] However, the samples are synthesized with long time and complex processes.

In this study, we used the idea of reactive porogen to modify a common high temperature porogen,

polystyrene, and synthesize mesoporous low-*k* films. We proposed a mesoporous organosilicate by using TEPSS and MSQ as reactive porogen and matrix to minimize porogen aggregation at high porosity. The TEPSS reactive porogen in this study include some characteristics such as polymer synthesize simply, controllable molecular weight (MW), and high reactive with matrix. To identify this novel low-*k* material, we first examined the structures and thermal characteristics of TEPSS reactive porogen and TEPSS-MSQ [*i.e.* triethoxy(polystyrene)silane-g-poly(methyl -silsesquioxane)], respectively. In addition, the morphology, pore size, the porosity, and dielectric of porous MSQ low-*k* film were investigated and discussed.

## 研究方法

**Materials. --** Styrene (St) (Acros, 99%) was distilled and stored at 5 °C. Copper(I) bromide (CuBr(I)) (Sterm Chemicals, 98%) was sublimated before using and stored at 15 °C. Methyltrimethoxysilane (MTMS) (Acros, 97%), *N,N,N*',*N*",*N*"-pentamethyl- diethylenetriamine (PMDETA) (Acros, 99$^{+}$%), hexafluorophosphoric acid ($HPF_6$) (Acros, 60 wt%), (3-chloropropyl)(triethoxy)silane (CPTES) (TCI, 95%), and sodium laurylsulfate (SDS) (SHOWA, 90$^{+}$%) were used as-received. Dimethylformamide (DMF) (Aldrich, 99%) and tetrahydrofuran (THF) (Echo, 99%) were distilled to keep them anhydrous before use. Toluene (Aldrich, 99.8%) and *p*-xylene (Aldrich, 99%) were used as-received.

**Synthesis of triethoxy(polystyrene)silane (TEPSS) using ATRP reaction. --** CuBr(I) (2.0 mM) was added to a 100 mL two-necked flask equipped with a magnetic stirring bar and a condenser. After sealing, the flask was degassed for 2 hours. The initiator, (CPTES, 1.0 mM), solvent (*p*-xylene, 4 mL), or styrene (50.0 mM) was degassed individually by three freeze-pump-thaw cycles for each. Subsequently, *p*-xylene, the catalyst (PMDETA, 2.0 mM), CPTES, and styrene were transferred into a flask, which was immediately sealed under argon. The mixture in the flask was placed in an oil bath and stirred at 80 °C for 12 hours under argon atmosphere. At the end of the polymerization reaction, the flask was quenched in cold water, subsequently diluted with THF. Afterwards, $Cu^{2+}$ was removed through an alumina column. The solvent was evaporated under reduced pressure, and the product was TEPSS with a yield of 58.6%.

**Synthesis of poly(methylsilsesquioxane) (MSQ) using sol-gel reaction. --** Methyltrismethoxysilane (MTMS, 24.0 mM), distilled water (DI water) (18.0 mM), and hexafluorophosphoric acid solution ($HPF_6$) (0.3 mM) were added into an aluminum dish, which was then heated in an oven at 80 °C for 3.5 minutes.

**Grafting TEPPS onto MSQ through sol-gel reaction. --** TEPSS ($2.9\times10^{-3}$ mM) and SDS ($3.5\times10^{-3}$ mM) were first dissolved by 6 mL THF in a 100 mL flask. Afterwards, MSQ (1.6 mM) was added into the flask, and then 0.06 g of dilute HCl (10%) was added into the flask slowly. The mixture was carried out at 50 °C in an oil bath under $N_2$ atmosphere for 6 hours. The sol-gel grafting reaction product was named TEPSS-MSQ. The TEPSS loading was varied from 0.6% to 6.6% to increase the loading of high-temperature reactive porogen.

**Preparation of porous low-*k* film. --** TEPSS-MSQ was dissolved in a chosen solvent, THF, to form a 20 wt% solution. The solution was first filtered through a 0.2 μm PTFE filter (Millipore Inc.), and then spun onto a (100) silicon wafer at 2000 rpm for 30 seconds. The TEPSS-MSQ film was subsequently baked at 100 °C for 1 minute, and then cured on a hot plate preheated at 250 °C for 30 minutes to form a crosslinked MSQ structure. The TEPSS reactive porogens were thermally decomposed at 400 °C for 90 minutes to form a porous low-*k* MSQ films. The nominal thickness of TEPSS-MSQ film cured at 250 °C is 280 nm, unless specified otherwise.

**Measurements.** -- The chemical structures of TEPSS and TEPSS-MSQ were validated by $^{1}$H-NMR spectra and $^{29}$Si-NMR spectra. $^{1}$H-NMR spectra [Bruker AC-300P (300 MHz)] were recorded in solution, with the tetramethylsilane (TMS) proton signal as an internal standard. $^{29}$Si-NMR spectra for powder samples were carried out by a Bruker DSX-400WB NMR spectrometer. The number-average ($M_n$), weight-average ($M_w$) molecular weight, and the molecular weight distribution (*i.e.* polydispersity index, PDI) were determined by gel permeation chromatography (GPC) using a Waters Chromatography unit interfaced with a Water 2414 differential refractometer (Waters Corporation, Ashland), and using tetrahydrofuran (THF) as an eluant and polystyrene as standard. TGA Q500 (TA Instruments) was used to measure the decomposition temperature of TEPSS and TEPSS-MSQ. The temperature scan speed was 10 °C/min from 100 °C to 700 °C under a nitrogen atmosphere.

The density of porous MSQ film was measured by X-ray reflectivity (XRR). The films were scanned by a Bruker D8 Discover with Cu $K_\alpha$ source ($\lambda$=0.154 nm) using $\omega$-2$\theta$ method with 2$\theta$ from 0° to 2°. Porosity (P) was then calculated by the Eq. (1):

$$\rho=\rho_s(1-P) \quad (1)$$

where $\rho$ is film density (g/cm$^3$), $\rho_s$ is silica density (1.63 g/cm$^3$). The sizes of the porogen in the hybrid low-*k* films were then characterized by GISAXS. GISAXS data were collected by using Beamline 23A1 of the National Synchrotron Radiation Research Center (NSRRC), Hsinchu, Taiwan. All of the GISAXS data were obtained using an area detector that covered a scattering wave vector ($q$) range from 0.015 to 0.025 Å$^{-1}$, and the incident angle of the X-ray beam (0.5 mm diameter) was fixed at 0.2° with an X-ray energy of 10 keV. Then, the pore size was analyzed by a sphere model using Guinier's law.[31,32]

The topography of porous film was examined by using a dual beam FIB/SEM (Nova Nanolab 2000 system, FEI Company) system. The film thicknesses of TEPSS-MSQ and porous MSQ film were measured using n&k Analyzer 1280 (n&k Technology, Inc.) at wavelengths ranging from 190 to 900 nm. The dielectric constant ($k$) of porous low-*k* films were measured by C-V dots (HP 4280, HP) with a sweeping frequency of 1 MHz based on a MIS configuration [Al electrode/low-*k* film/Si (50 ohm-cm)] at room temperature.

## 結果與討論

**Characterization of TEPSS.** -- The synthesis of TEPSS using ATRP reaction is schematically illustrated in Figure 1. CuBr(I) metal center undergoes an electron transfer with simultaneous halogen atom abstraction and expansion of its coordination sphere, which activates the initiator, CPTES for the free-radical polymerization.[33] The chemical structure of TEPSS was validated by $^{1}$H-NMR spectrum as shown in Figure 2(a). There are two characteristic signals associated with styrene: (1) the peaks in the 6.45-7.18 ppm range representing the aryl protons of styrene units and (2) the signals in the range of 1.25-1.84 ppm assigned to the methylene protons of styrene backbone. Moreover, signals at 3.7 ppm are attributed to siloxane (-Si-$(OCH_3)_3$) end group. Since the siloxane group represents initiator characteristic, it can be used as a model to study the starting of polymerization. Hence, based on $^{1}$H-NMR spectrum, TEPSS has been successfully synthesized by ATRP.

Next, the decomposition temperature of reactive porogen, TEPSS was characterized by thermogravimetric analysis (TGA) to determine the maximum processing temperature of TEPSS-based low-*k* films in the late porogen removal scheme. Figure 2(b) showed the dynamic TGA curve of TEPSS from 100 °C to 800 °C. The decomposition temperature ($T_d$) is 362 °C, at which 5% weight-loss occurs, and the weight

loss is attributed to the decomposition of the PS long-chains in TEPSS. PS long-chains could be removed at T > 435 °C under $N_2$ atmosphere in dynamic mode at heating rate of 10 °C/min. Meanwhile, PS long-chains also could be completely removed at 400 ˚C isothermally for 1 hour under a $N_2$ atmosphere. As the result, reactive porogen, TEPSS, can be used in conventional back-end fabrication processes and can be burn out completely without issue.

**Molecular weight control of TEPSS. --** For low-*k* dielectric applications, one prefers a low-molecular weight TEPSS in order to obtain smaller porogen size in the low-*k* matrix/porogen mixture, thereby smaller pore size in the porous low-*k* materials after the removal of porogen through thermal decomposition. Furthermore, the control of molecular weight distribution is highly desirable to obtain tight pore size distribution. We first selected a solvent among toluene, *p*-xylene, and DMF for achieving TEPSS with a lower molecular weight using ATRP method at fixed CPTES initiator concentration ($1x10^{-4}$ mole) and time (1000 minutes). Then the dependence of TEPSS molecular weight on the CPTES initiator concentration in the fixed solvent was examined.

The measured molecular weights ($M_n$ and $M_w$) and polydispersity index (PDI) of TEPSS under various synthesis conditions (*i.e.* CPTES initiator concentration and different solvents) using ATRP method are summarized in Table 1. Firstly, it is found that TEPSS had the largest molecular weight ($M_n$: 81,400 g/mole) when DMF solvent was used. TEPSS molecular weight was decreased to 28,000 g/mole when toluene was used as the solvent. In contrast, *p*-xylene solvent yielded TEPSS with the smallest molecular weight (26,100 g/mole). The difference in the molecular weight of TEPSS by various solvents can be attributed to the solubility parameter between the solvent and the CPTES initiator. In specific, the solubility parameters of CPTES, DMF, toluene, and *p*-xylene are 7.44, 10.6, 8.9 and 7.0, respectively.

For ATRP reaction occurring in solution, the general expression for the rate of polymerization ($R_M$) is given by $R_M = \kappa_p[IM\bullet][M]$, where [IM•] represents the concentration of the growing chains, and [M] is the concentration of the monomer.[34] The equation illustrated that the concentration of the growing chains can affect the reaction rate. The CPTES initiator was dissolved in *p*-xylene effortlessly due to it have closer solubility parameter to *p*-xylene. Therefore, the reaction solution may have more growing chains and can increase the termination rate when *p*-xylene was used as solvent. The polymer molecular weight can be decreased while more growing chains were grew and increasing the termination rate.[35]

Table 1 also shows the effect of CPTES initiator concentration on the molecular weight of TEPSS. It was found that the molecular weight of TEPSS decreased from 26,100 g/mol to 3,500 g/mol with increasing CPTES initiator concentration from $1\times10^{-4}$ mole to $4\times10^{-4}$ mole. The relationship between initiator concentration and polymer molecular weight in ATRP method can be described by Eq. (2):[36]

$$\ln\frac{[M]_0}{[M]} = A[I] \qquad (2)$$

where $A=k_p K t [Cu^+][Cu^{2+}]^{-1}$ as a constant, $K = k_a/k_d$, $k_a$ represented the rate constant for activation, and $k_d$ was rate constant for deactivation. From the equation, it can be observed that the relationship between polymer molecular weight and the initiator concentration was inverse proportion. Due to the numbers of radical were increased when the concentration of initiator was increased,[37] and the rate of polymerization would become faster when there were more radical, and caused smaller polymer molecular weight.

Overall, we found that both solvent and initiator played critical roles in controlling the molecular weight of TEPSS using ATRP technique. Solvent with solubility parameter close to the CPTES initiator increases the

dissolution of the initiator and thus the initiator concentration in the solution. The increased initiator concentration led to a smaller molecular weight of TEPSS. In addition, the low PDI of TEPSS for all cases in Table 1 (PDI ≤1.17) shows tight molecular weight distribution owing to ATRP synthesis technique. As the result, TEPSS with 3500 g/mole molecular weight and *p*-xylene solvent were selected for the synthesis of reactive porogen at a fixed initiator concentration for the rest of this paper.

**Characterization of TEPSS-MSQ.** -- In this study, the MSQ low-*k* matrix was synthesized from MTMS monomer by sol-gel process as illustrated in Figure 3(a). MSQ as oligomer has silanol groups on the end caps, which facilitates the grafting reaction of TEPSS onto MSQ matrix by sol-gel reaction. This yielded a TEPSS-grafted-MSQ copolymer named TEPSS-MSQ as schematically illustrated in Figure 3(b).

This approach is to take advantage of the narrow PDI of reactive porogen, TEPSS in order to obtain the porous low-*k* films with tight pore distribution even at high porosity. It is essential to validate the success of grating reaction by examine the neighboring groups and chemical environment surrounding Si using $^{29}$Si-NMR spectroscopy. Figure 4 shows the solid state $^{29}$Si-NMR spectra of MSQ and TEPSS-MSQ. The $^{29}$Si-NMR spectrum of MSQ shows a $T^3$ signal at -69 ppm, which represents three Si-O- bonds and one alkyl group, R, [$(SiO)_3Si^*R$] species.[38,39,40] Besides, a $T^2$ signal at -56 ppm, which refers to the silicon nuclei with hydroxyl group termination, [$(SiO)_2Si^*(OH)(CH_3)$] species. In comparison, the spectrum of TEPSS-MSQ shows two signals at -54 ppm ($T^2$) and -69 ppm ($T^3$) with different intensities. The relative intensity ratio of $T^3$:$T^2$ in TEPSS-MSQ is ~9.3, which is significantly higher as compared to 3.1 of pure MSQ. The increase can be attributed to two factors. First, a MSQ network structure with [$(SiO)_3Si^*CH_3$] groups ($T^3$) was formed via the condensation reaction of the silanol groups in MSQ, typically in the form of [$(SiO)_2Si^*(OH)(CH_3)$], whose signal was originally at -56 ppm ($T^2$). The other source for increased $T^3$ groups involved the grafting reaction between TEPSS and MSQ through hydrolysis and condensation. In contrast, when TEPSS is grafted onto MSQ, $T^2$ signal was down shifted from -56 ppm to -54 ppm, which is presumably due to a the formation of a $T^2$ group through the condensation reaction of TEPSS and MSQ with 2 hydroxyl sites. In addition, the downshift was attributed to the electron-withdrawing by the polystyrene group in TEPSS.[41] However, the results of $^{29}$Si-NMR is still not conclusive in the confirmation of the grafting of TEPSS onto MSQ via sol-gel reaction.

**Thermal decomposition and characteristics.** -- Therefore, the thermal characteristics such as thermal stability and decomposition temperature of starting MSQ and reaction product, TEPSS-MSQ (the ratio of TEPSS to MSQ: 10%), were examined to further confirm the grafting reaction between TEPSS and MSQ by dynamic TGA as shown in Figure 5. Pure MSQ showed a high thermal stability, a mere 2.5% weight loss over a range between 200 °C and 700 °C. In contrast, TEPSS-MSQ showed slightly less thermal stability between 350 °C and 500 °C. Specifically, there was additional 1% weight loss from 376 °C to 460 °C for TEPSS-MSQ. Such weight loss was considered to arise from the decomposition of the polystyrene (PS) long chain in TEPSS. Also, the thermal decomposition temperature ($T_d$) of PS long chain in TEPSS grafted onto MSQ was calculated at 383 °C, which is almost 20 °C higher than the $T_d$ (362 °C) of TEPSS discussed in aforementioned section. The increased $T_d$ of PS in TEPSS-MSQ is primarily caused by the confinement effect by the MSQ network structure at T > 350 °C. The combined results by $^{29}$Si-NMR, FTIR, and TGA confirmed that the reactive porogen, TEPSS has been successfully grafted onto MSQ.

**Pore Morphology and pore size of porous MSQ films with different porosities. –** After coating of TEPSS-MSQ thin film, the reactive porogen, TEPSS, was thermally removed to form porous MSQ film. The

porosity was controlled by adjusting the weight ratio of TEPSS to MSQ and measured by XRR. In addition, the pore sizes were characterized by GISAXS measurement. Table 2 summarizes the density, porosity, dielectric constant, and pore size with different TEPSS loading. As TEPSS loading increased from 0.6% to 6.6%, the porosity of porous MSQ films was increased from 18% to 54% and the density was reduced from 1.27 g/cm$^3$ to 0.71 g/cm$^3$ after 400 °C curing. After the thermal decomposition of PS long chains at 400 °C, the pore morphology of porous low-*k* MSQ films with various porosities were first examined by SEM and shown in Figures 6(a) through 6(d) for 18%, 23%, 31%, and 54% porosity, respectively. Porous MSQ films at porosities up to 54% were found to be continuous and smooth with small pores (< 20 nm) in fairly random distribution. In addition, the shape of pores is nearly a sphere without obvious aggregation. This indicates that the reactive porogen grafting scheme (*i.e.* TEPSS grafted onto MSQ) can yield smaller pores and uniform distribution.

However, in order to quantify the pore size precisely, GISAXS measurements were further carried out for such porous MSQ films. In our case, the 2D scattering patterns were analyzed by a particulate system which treats the pores in the matrix the same as the particles in the films. It is known that the intensity of scattering pattern ($I_{(q)}$) is proportional to the product of intra-particle structure factor ($P_{(q)}$, form factor) and inter-particle structure factor ($S_{(q)}$, structure factor) as expressed by Eq. (3)

$$I_{(q)} \propto P_{(q)} \cdot S_{(q)} \tag{3}$$

where $q$ is the scattering wave vector defined by scattering angle ($\theta$) and wavelength of radiation ($\lambda$) of x-ray by Eq. (4):

$$q = \frac{4\pi}{\lambda} \cdot \sin\theta \tag{4}$$

The structure factor $S_{(q)}$ is close to one in a low-concentration system or a system without inter-particle interactions, and thus can be ignored. Hence, the scattering intensity distribution for a polydisperse system is proportional to the ensemble average of the form factor ($P_{(q)}$) which has been evaluated for a variety of particle shapes (spheres, rods, discs etc.). However, in the range of very low $q$-value ($q << 1$), $P_{(q)}$ can be generalized for a spherical particle system by using the Guinier approximation[42,43,44,45] with a radius of gyration ($R_g$), and then Eq.(3) can be further derived as Eq.(5):

$$I_{(q)} \propto \exp\left(\frac{-q^2 R_g^2}{3}\right) \tag{5}$$

Hence, a linear relationship exists between $\ln I_{(q)}$ and $q^2$, with a slope of ($-R_g^2/3$), and the steeper the slope, the larger the radius.

Figure 7 shows the Guinier plot ($\ln I_{(q)}$ *vs.* $q^2$) for porous MSQ films with different porosities, which were extracted from MSZ film scattering pattern and approximated by Guinier theory for quantitative analysis. The similar slopes indicate that the $R_g$ size was maintained with the porosity increasing from 18% to 31%. The slope changed varied little when the porosity was up to 54%. Since the shape of pore is close to a sphere as confirmed by SEM, the pore diameter ($d$) could be deduced from $d = 2\times(5/3)^{1/2}\times R_g$.[46,47] As a result, the pore size maintained 18 nm with porosity increasing from 18% to 31%, but showed little variation that pore size was increased to 19 nm at 54% porosity. Consequently, grafting reactive porogen onto low-*k* matrix can cause small pore and has less pore aggregation below a critical porosity, *i.e.* ~31% porosity for TEPSS-MSQ system.

However, the reactive TEPSS porogen loading is not only affect the pore size, but also affect the dielectric constant of low-*k* films after porogen removal due to the dielectric constant of air is 1.0. Therefore, the relationship between the porosity (TEPSS loading) and dielectric constant will be discussed in the following section.

**Dielectric property of porous MSQ low-*k* film. --** In order to understand the dielectric properties of such porous MSQ films with various porosity, all samples were examined using the CV-dot measurements. At first, the dielectric constant of pure MSQ film was measurement ($k_{MSQ}$ = 2.81). Afterward, the dielectric constants of porous MSQ films with different porosities were measurement and also tabulated in Table 2. Compared with pure MSQ film, the dielectric constant of the porous MSQ film with 18% porosity decreased to 2.59 and even lower to 2.30 when porosity increased to 54%. On the other hand, the calculated values of porous TEPSS-MSQ films were higher than theory values. This is due to the porous MSQ films have absorbed water during the test, and water has extremely polar -OH bonds and its *k*-value close to 80. Therefore, even a small amount of absorbed water can increase the total *k*-value.[48] Consequently, this paper decreased the dielectric constant of porous MSQ effectively by increasing the loading of TEPSS form 2.81 to 2.30 at 54% porosity.

## 結論

This study introduced a novel method for preparing a mesoporous low-*k* material, TEPSS-MSQ, by using a reactive high-temperature porogen, TEPSS, suitable for a late-porogen removal integration scheme. As results, the molecular weight of TEPSS could be controlled by the concentration of initiator and the reaction solvents. In this study, *p*-xylene was demonstrated to be the most suitable solvent which can decrease the TEPSS molecular weights (3,500 g/mole) largely. Afterward, molecular weights, chemical structure, and thermal characteristics of TEPSS were indicated by GPC, $^{1}$H-NMR, and TGA, respectively. In addition, the extremely low polydispersity by using ATRP and controllable reactivity of TEPSS with MSQ matrix yielded uniformly distributed and spherical pores (~18 nm) with less aggregation at 31% porosity. However, pore size is slight increased to 19 nm at 54% porosity investigated by GISAXS analysis. Furthermore, the dielectric constant of porous MSQ film is decreased to 2.37 and 2.30 when porosity reached to 31% and 54%.

**附表**

Table 1. The synthesis parameters (initiator concentration, solvents, reaction time), the molecular weights ($M_n$ and $M_w$), and PDI of TEPSS

| [I] ($10^{-4}$ mole) | Solvent | Time (min) | $M_n$ (g/mole) | $M_n$ (g/mole) | PDI |
|---|---|---|---|---|---|
| 1.0 | DMF | 1000 | 81,400 | 95,800 | 1.17 |
| 1.0 | Toluene | 1000 | 28,000 | 30,300 | 1.08 |
| 1.0 | *p*-xylene | 1000 | 26,100 | 27,800 | 1.06 |
| 2.0 | *p*-xylene | 1000 | 8,800 | 9,900 | 1.13 |
| 4.0 | *p*-xylene | 1000 | 3,500 | 3,900 | 1.12 |
| | | | [I]:[St]:[CuBr]:[PMDETA]=1:500:20:20 (in first condition) | | |

Table 2. The density, porosity, pore size, and dielectric constant of porous MSQ films with different porosity

| TEPSS loading (%) | Density (g/cm$^3$) | Porosity (%) | Dielectric constant ($k$) | Pore size (nm) |
|---|---|---|---|---|
| 0 | 1.54 | 0% | 2.81 | - |
| 0.6 | 1.27 | 18% | 2.59 | 18 |
| 1.3 | 1.18 | 23% | 2.45 | 18 |
| 3.3 | 1.07 | 31% | 2.37 | 18 |
| 6.6 | 0.71 | 54% | 2.30 | 19 |

**附圖**

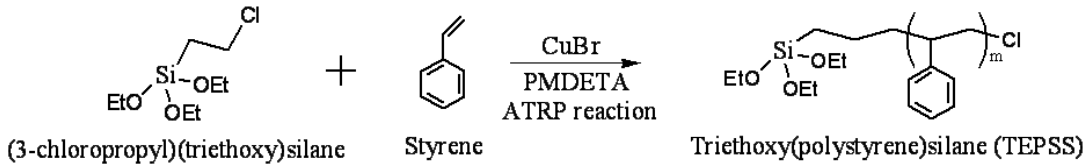


Figure 1. Model reaction for the synthesis of TEPSS by ATRP.

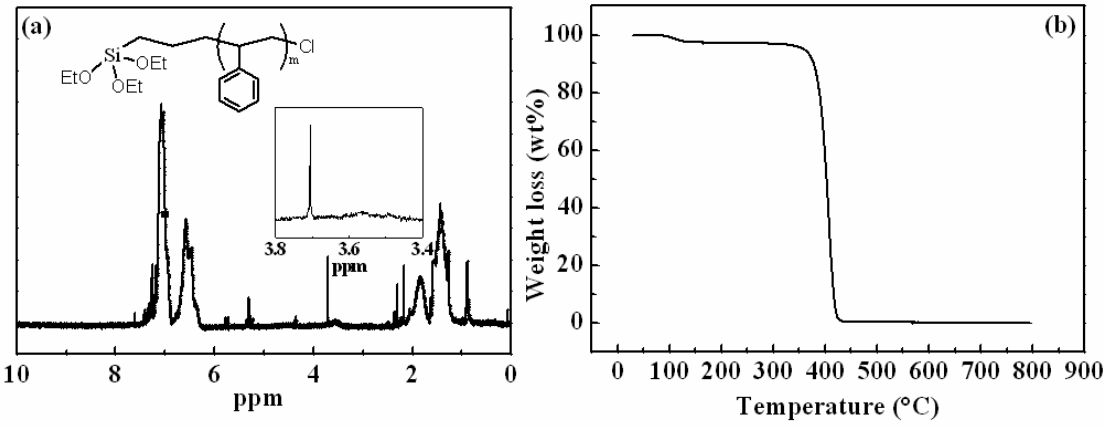


Figure 2. The properties of TEPSS. (a) $^1$H-NMR spectra, and inset shows the Si-$(OCH_3)_3$ data in the rage of 3.4 to 3.6 ppm, and (b) the dynamic TGA thermogram from 100 °C to 800 °C.

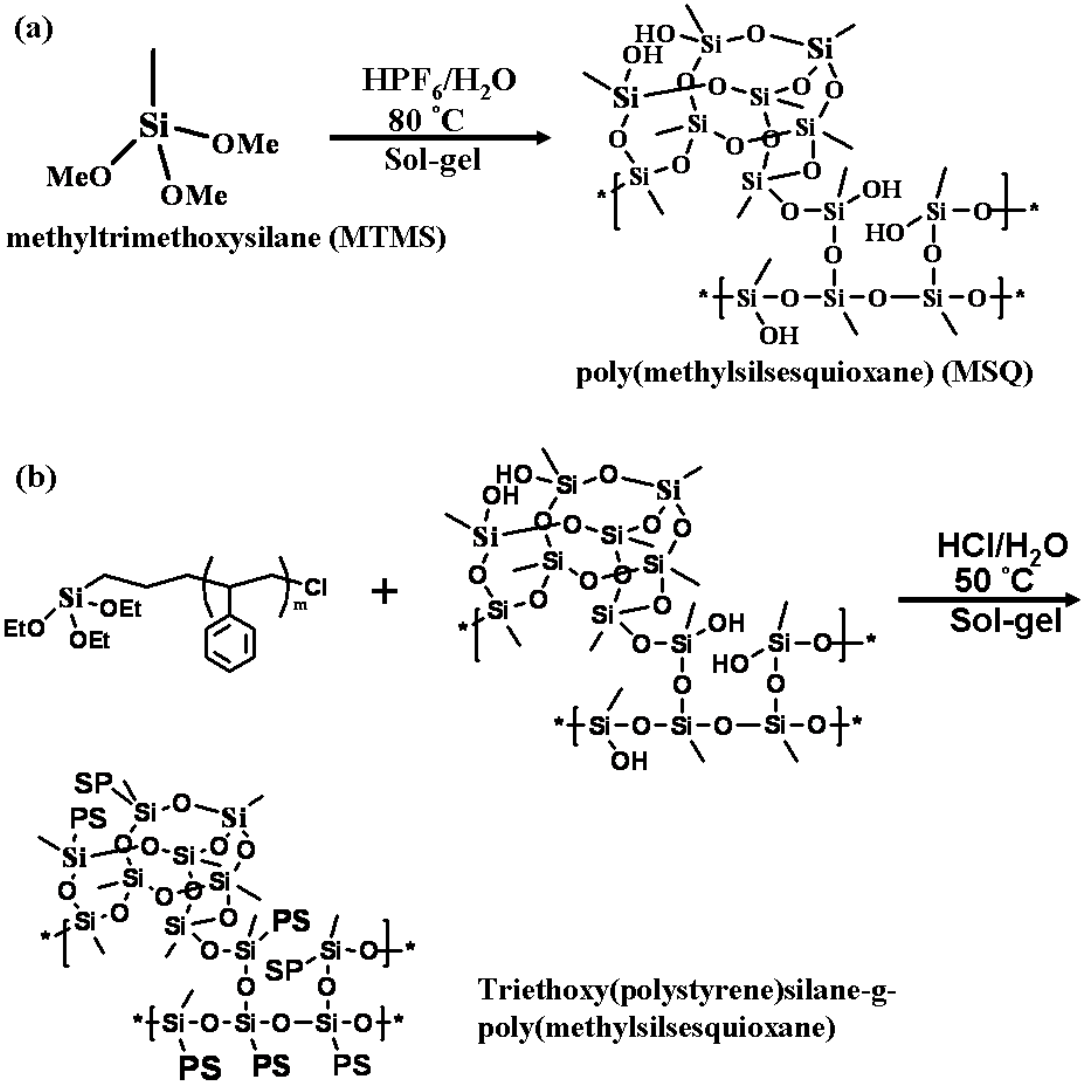


Figure 3. The synthetic schematic of TEPSS-MSQ: (a) synthesis of MSQ from MTMS by sol-gel method, and (b) TEPSS-MSQ was synthesized by grafting TEPSS onto MSQ.

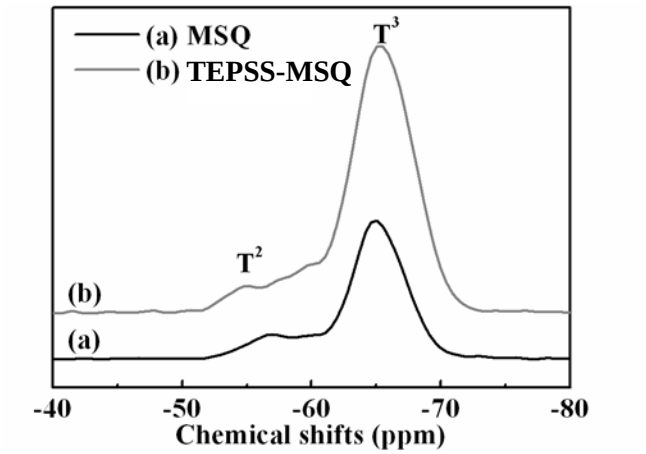


Figure 4. The $^{29}$Si-NMR spectra of (a) MSQ and (b) TEPSS-MSQ cured at 60°C.

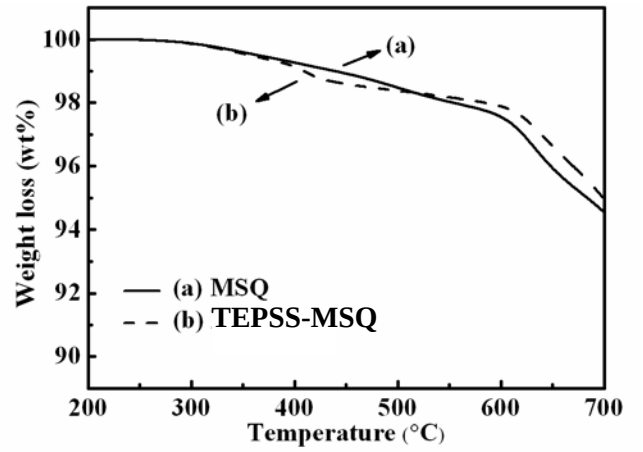


Figure 5. The dynamic TGA thermogram of (a) MSQ and (b) TEPSS-MSQ.

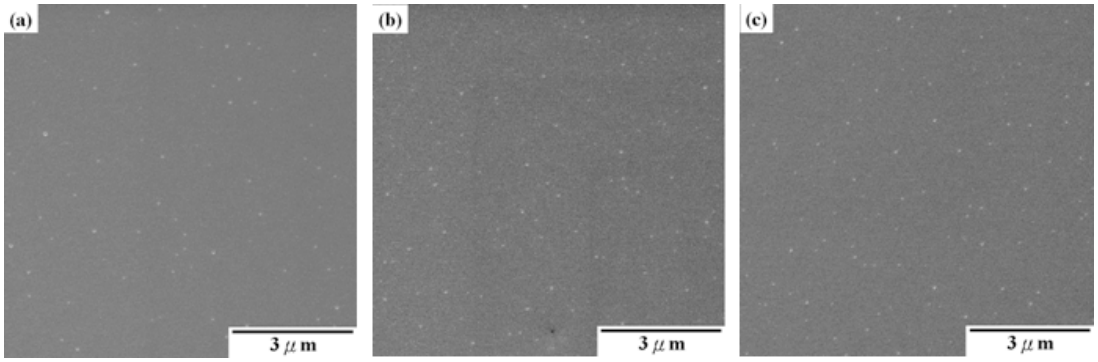


Figure 6. SEM photograph of porous TEPSS-MSQ film in different porosity: (a) 18%, (b) 23%, (c) 31%

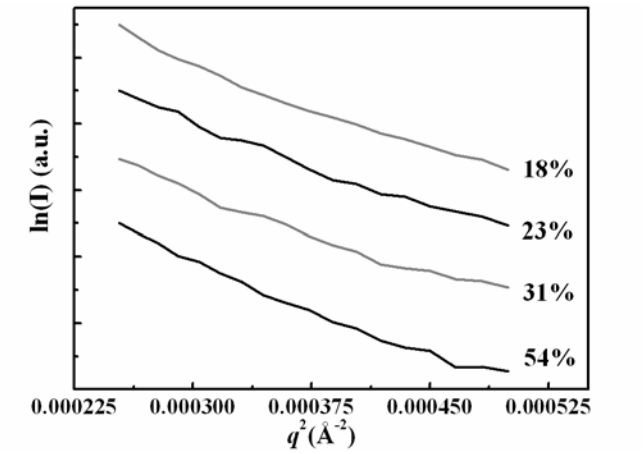


Figure 7. ln($I$)-$q^2$ plots from 2D GISAXS scattering patterns of TEPSS-MSQ films with different porosity.

## 參考文獻


1 M. Bohr, Tech. Digest IEEE Int. Electronic Device Meeting (1995).

2 C. H. Jan, Short Course on Low-k dielectrics, IEEE Int. Electronic Device Meeting (2003).

3 D. Edelstein, J. Heidenreich, R. Goldblatt, W. Cote, C. Uzoh, N. Lustig, R. Roper, T. McDevitt, W. Motsiff, A. Simon, J. Dukovic, R. Wachnik, H. Rothore, R. Schulz, L. Su, S. Luce, and J. Slattery, in IEEE Int. Electron Device Meeting, 773 (1997).

4 International Technology Roadmap for Semiconductors, Executive Summary (2005).

5 Y. H. Wang and R. Kumar, *J. Electrochem. Soc.*, **151**, 73 (2004).

6 K. Endo, K. Kishimoto, Y. Matsubara, and K. Koyanagi, Chapter 5 "Plasma-enhanced chemical vapor deposition of FSG and a-C:F low-k materials," pp121-166, in Low Dielectric Constant Materials for IC Applications, eds P. S. Ho, J. Leu, and W. W. Lee, Springer (2002).

7 S. Yang, S. Ahmed, B. Acrcot, R. Arghavani, P. Bai, S. Chambers, P. Charvat, R. Cotner, R. Gasser, T. Ghani, M. Hussein, C. Jan, C. Kardas, J. Maiz, P. McGregor, B. McIntyre, P. Nguyen, P. Packan, I. Post, S. Sivakumar, J. Steigerwald, M. Taylor, B. Tuff, S. Tyagi, and M. Bohr, in Int. IEDM '98 Technical Digest 197 (1998).

8 X. Y. Bao, X. S. Zhao, X. Li, and J. Li, *Appl. Surf. Sci.*, **237**, 380, (2004)

9 P. Verdonck, D. De Roest, S. Kaneko, R. Caluwaerts, N. Tsuji, K. Matsushita, N. Kemeling, Y. Travaly, H. Sprey, M. Schaekers, and G. Beyer, *Surf. Coat. Technol.*, **201**, 9264 (2007).

10 S. Malhouitre, C. Jehoul, J. V. Aelst, H. Struyf, S. Brongersma, L. Carbonell, I. Vos, G. Beyer, M. V. Hove, D. Gronbeck, M. Gallagher, J. Calvert, and K. Maex, *Microelectron. Eng.*, **70**, 302 (2003)

11 M. Che, and J. Leu, in IEEE Int. Electron Decices and Materials Symposia, oral section AO-417 (2008).

12 H. J. Lee, C. L. Soles, B. D. Voqt, D. W. Liu, W. L. Wu, E. K. Lin, H. C. Kim, V. Y. Lee, W. Volksen, and R. D. Miller, *Chem. Mat.*, **20**, 7390 (2008)

13 A. Zenasni, F. Ciaramella, V. Jousseaume, C. Le Cornec, and G. Passemard, *J. Electrochem. Soc.* **154 (1)**, G6 (2007).

14 J. F. Lutz, and K. Matyjaszewski, *Macromol. Chem. Phys.*, **203**, 1385 (2002).

15 K. Matyjaszewski, and J. Xia, *Chem. Rev.*, **101**, 2921 (2001).

16 B. Lee, J. Yoon, W. Oh, Y. Hwang, K. Heo, K. S. Jin, J. Kim, K. W. Kim, and M. Ree, *Macromolecules*, **38**, 3395 (2005).

17 J. N. Sun, Y. Hu, W. E. Frieze, W. Chen, and D. W. Gidley, *J. Electrochem. Soc.*, **150**, F97 (2003).

18 J. Calvert and M. Gallagher, *Semicond. Int.*, **26**, 52 (2003).

19 M. L. Che, C. Y. Huang, S. Choang, Y. H. Chen, and J. Leu, *J. Mater. Res.,* **25**, 1049 (2010).

20 J. Kovacik, *J. Mate. Sci. Lett.*, **18**, 1007 (1999).

21 J. T. Wetzel, S. H. Lin, E. Mickler, J. Lee, B. Ahlbum, C. Jin, R. J. Fox III, M. H. Tsai, W. Mlynko, K. A. Monnig, and P. M. Winebarge, IEEE IEDM, 73 (2001).

22 J. P. Hsu, S. H. Hung, and W. C. Chen, *Thin Solid Films,* **473,** 185 (2005).

23 Y. Oku, K. Yamada, T. Goto, Y. Seino, A. Ishikawa, T. Ogata, K. Kohmura, N. Fujii, N. Hata, R. Ichikawa, T. Yoshino, C. Negoro, A. Nakano, Y. Sonoda, S. Takada, H. Miyoshi, S. Oike, H. Tanaka, H. Matsuo, K. Kinoshita, and T. Kikkawa, 2003 IEDM, O3-139 (2003).

24 Y. Chen, and J. Leu, *2008 MRS Fall Meeting*, 510449 (2008).

25 C. V. Nguyen, K. R. Carter, C. J. Hawker, J. L. Hedrick, R. L. Jaffe, R. D. Miller, J. F. Remenar, H. W.

Rhee, P. M. Rice, M. F. Toney, M. Trollss, and D. Y. Yoon, *Chem Mater.*, **11**, 3080 (1999).
26 B. Lee, W. Oh, J. Yoon, Y.Hwang, J. Kim, B. G. Landes, J. P. Quintana, and M. Ree, *Macromolecules*, **38**, 8991 (2005).
27 K. Heo, K. S. Jin, W.Oh, J. Yoon, S. Jin, and M. Ree, *J. Phys. Chem. B*, **110**, 15887 (2006).
28 A. Heise, J. L. Hedrick, M. Trollss, R. D. Miller, and C. W. Frank, *Macromolecules*, **32**, 231 (1999).
29 A. Heise, C. V. Nguyen, R. Malek, J. L. Hedrick, C. W. Frank, and R. D. Miller, *Macromolecules*, **33**, 2346 (2000).
30 B. Lee, W. Oh, Y. Hwang, Y. H. Park, J. Yoon, K. S. Jin, K. Heo, J. Kim, K. W. Kim, and M. Ree, *Adv. Mater.*, **17**, 696 (2005).
31 Y. H. Lai, Y. S. Sun, U. Jeng, J. M. Lin, T. L. Lin, H. S. Sheu, W. T. Chuang, Y. S. Huang, C. H. Hsu, M. T. Lee, et al., *J. Appl. Crystallogr.*, **39**, 871 (2006).
32 R. J. Roe, *Methods of X-Ray and Neutron Scattering in Polymer Science*, Chap. 5, Oxford University Press, New York (2000).
33 G. Odian, *Principles of Polymerization*, 4th ed., p. 316, Wiley Interscience, New York (2004).
34 G. T. Lewis, V. Nguyen, and Y. Cohen, *J Polym Sci Part A: Polym Chem*, **45**, 5748 (2007).
35 E. Grau, J. P. Broyer, C. Boisson, R. Spitz, and V. Monteil, *Macromolecules,* **42,** 7279 (2009).
36 H. Fischer, *J Polym Sci Part A: Polym Chem*, **37**, 1885 (1999).
37 K. Matyjaszewski, J. L. Wang, T. Grimaud, and D. A. Shipp, *Macromolecules*, **31**, 1527 (1998).
38 L. Bourget, D. Leelereq, and A. Vioux, *J. Sol-Gel Sci. Technol.*, **14**, 137 (1999).
39 K. J. Shea, D. A. Loy, and O. Webster, *J. Am. Chem. Soc.*, **114**, 6700 (1992).
40 H. Jo and F. D. Blum, *Langmuir*, **15**, 2444 (1999).
41 K. Matyjaszewski and T. P. Davis, *Handbook of Radical Polymerization*, p. 140, John Wiley & Sons, Inc., New York (2003).
42 A. Guinier, Ann. *Phys.*, **12**, 161 (1939).
43 D. J. Kinning and E. L. Thomas, *Macromolecules*, **17**, 1712 (1984).
44 J. S. Pedersen, *J. Appl. Crystallogr.*, **27**, 595 (1994).
45 Y. Chen, U. Jeng, and J. Leu, *J. Electrochem. Soc.*, **158**, G52 (2011).
46 L. A. Feigin and D. I. Svergun, *Structure Analysis by Small Angle X-ray and Neutron Scattering*, Plenum, New York (1987).
47 A. Guinier and G. Fournet, *Small-Angle Scattering of X-rays*, John Wiley & Sons, New York (1955).
48 D. Shamiryan, T. Abell, F. lacopi, and K. Maex, *Materials Today*, **7**, 34 (2004).

# 國科會補助專題研究計畫項下出席國際學術會議心得報告

日期：100年05月13日

| | | | |
|---|---|---|---|
| 計畫編號 | NSC 99－2221－E－009－177－ | | |
| 計畫名稱 | 新穎接枝型起孔洞劑之多孔性低介電材料探討 | | |
| 出國人員姓名 | 呂志鵬 | 服務機構及職稱 | 國立交通大學 材料科學與工程學系 副教授 |
| 會議時間 | 100 年 05 月 01 日至 100 年 05 月 06 日 | 會議地點 | 加拿大 蒙特婁 |
| 會議名稱 | 第 219 屆美國電化學年會<br>219th Meeting of the Electrochemical Society | | |
| 發表論文題目 | 使用高溫起孔洞劑合成介孔洞低介電材料及其孔洞型貌與電性之探討<br>Synthesis, Pore Morphology, and Dielectric Property of Mesoporous Low-*k* Material PSMSQ Using a Reactive High-Temperature Porogen, TEPSS | | |

**報告內容如下：**

Trip Report –
ECS 219th Meeting, Montreal, Quebec, CANADA  Jim Leu

Photo Sessions

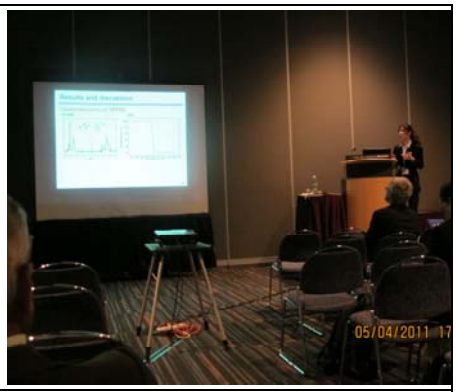

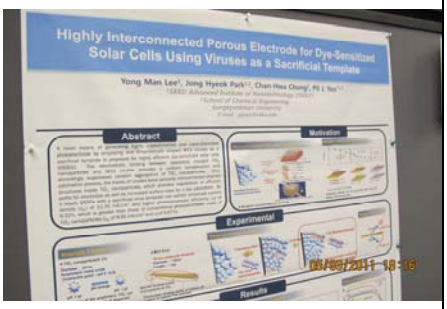


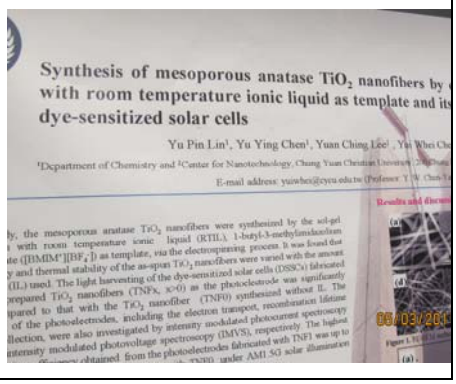


1. Useful information from Equipment and Materials Suppliers

(1) Catalogs from Gelest:

(a) reactive silicones, (b) Optical Materials, (c) hydrophobicity, hydrophilicity and silane surface modification, (d) metal-organic precursors, and (e) latest edition Silicon Compounds

You can find most of the catalogs except metal-organic precurors at their website: http://www.gelest.com/

(2) Request information from IFCON on the quartz crystals and QCM-R

**2. Technical summary**

1. The award seminar by Prof. S.J. Pearton

Gordon E. Moore Medal for Outstanding Achievement in Solid State Science and Technology Award Presentation

Wide Bandgap Semiconductors for Electronics, Photonics and Sensing Applications

By S.J. Pearton, Department of Materials Science and Engineering, University of Florida

Key learning from his talk can be summarized below

1. AlGaN/GaN-based devices as hydrogen sensors

Ohmic contact metal: (1) Ti/Al/Pt/Au, (2) Ti/Al/TiB2/Ti/Au

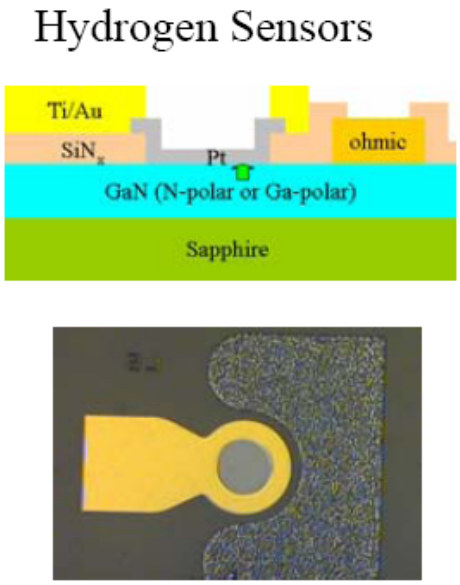




2. Semiconductor-based bio-sensors: biosensor consists of a bio-receptor and transducer. The bio-receptor is typically an enzyme or antibody layer attached to the gate of an FET

For example, the glucose oxidase enzyme catalyzes the reaction:

Glucose + O2 → gluconic acid + H2O2

The mechanism is to measure, for example, oxygen consumption, acid production, or hydrogen peroxide production

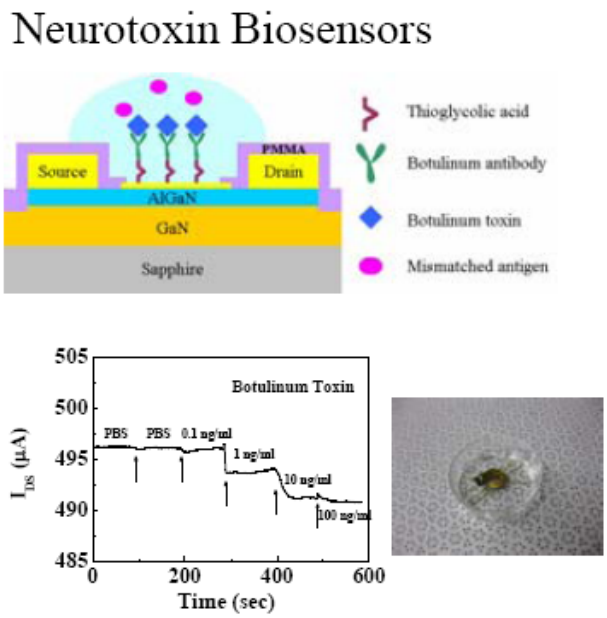

Some of research and development work on wide bandgap semiconductors:
Functionalization the sensor surface is critical

Bio-sensors that have been demonstrated include the following:
Toxins: botulinum
Cancers: prostate specific antigen (100 pg/l)
Breast cancer in saliva
Biomarkers in breath condensate
PH, Gluocose (0.5 nM)
Biomarkers in Buffer solutions
Lactic acid, chlorine ion etc.

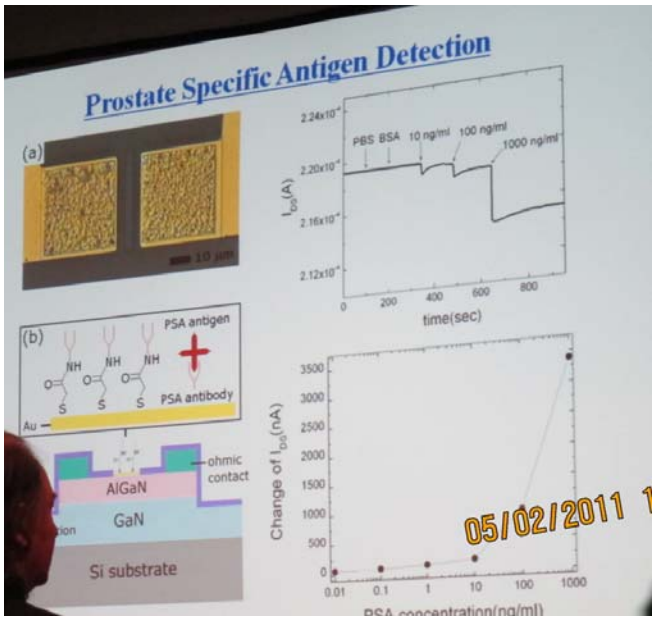


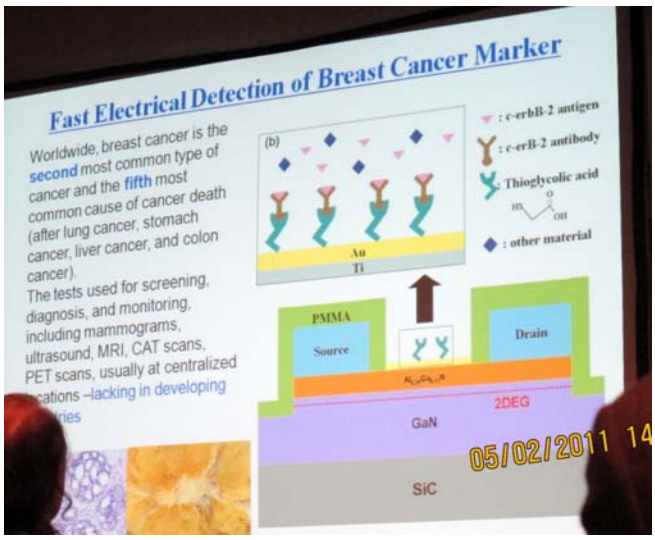

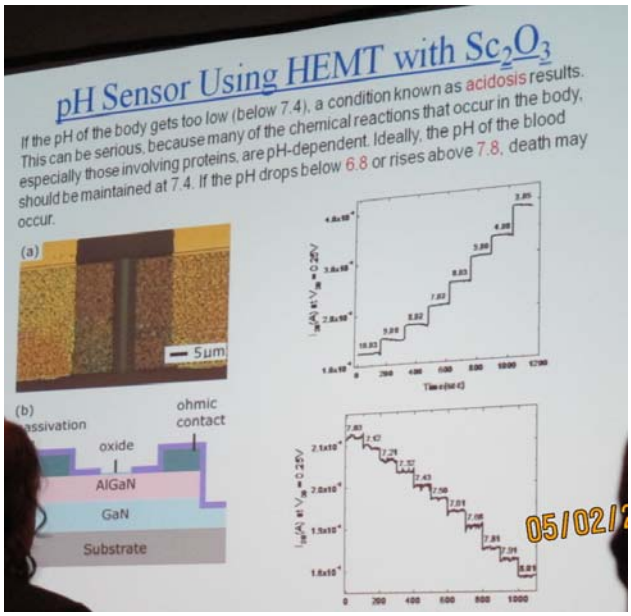


**DSSC**

1. Recipe for counter Pt electrode using electroless plating

(Abstract #1548) Optimization of electroless Pt counter electrodes for use in DSSCs by Yi-Ting Lin and Jeng-Yu Lin, Ta-Tung University

Me-EDA-Si grafted FTO glass; pH=4, Pt (0.5 M) Pt(111)

2. Abstract No. 63

Electrodeposited Pt counter electrode for DSSC using 3-(2-aminoethylamino)propyl-methyldiemthoxysilane as an additive

Che-Yu Lin et al. National Tsing Hua University

The efficiency of DSSC using electroplated Pt with Me-EDA-Si additive (5.86%) is comparable to that by sputter Pt (6.01%)

3. Highly interconnected Porous Electrode for DSSC using viruses as a sacrificial template

Yong Man Lee et al. Adv. Functional Materials, 21, 1160 (2011)

This is a very interesting poster paper, which turns out to be a high IF SCI paper published early this year. It appears to me that more and more presentation and posters are not true to the sprit of conference for sharing unpublished results.

4. Plasma treatment on FTO glass for DSSC (No. 1019) by S.-H. Kim et al.

from Chungnam National University

Plasma treatment enhances the bonding between TiCl4 layer and FTO. There is little change except better Voc.

5. (Abstract#260) Polymer electrolyte (PVDF-HPF) with mesoporous silica by Prof. Yui Whei Chen-Yang's group

   The addition of mesoporous silica (MSP) enhance the diffusivity of triiodide ~40%, thus the conductivity. There is a 37% increase in the efficiency

6. (Abstract #259) Synthesis of mesoporous anatase TiO2 nanofibers by electrospinning with room temperature ionic liquid and its application on DSSCs by Yu-Pin Lin et al, from Prof. Yui Whei Chen-Yang's group

1-D TiO2 fibers by electrospining using ionic liquid ([BMIM+][BF4-]) as template. The efficiency was increased to 5.61%.
Anatase phase, no rutile, surface area

7. Yu-Fan Su, Photocatalytic activities of nanostructure TiO2 photoeletrodes prepared using mild solvothermal method
   No explanation why TiCl4 treatment is critical, why rutile

8. No. 109 Ruet Toledano
   Eletrochemical deposition of sol-gel based nanohybrides (The Hebrew University of Jerusalem)

9. No. 106 Vaidyanathan Subramanian
   A new flexible quantum dot solar cell: Hetero structural mesh – TiO2 nanoparticles photosensitized with Cds

   http://pubs.acs.org/doi/abs/10.1021/ja0777741

   successive ionic layer adsorption and reaction (SILAR)
   Ultrasonic Assisted SILAR method (UA-SILAR) was developed and highly oriented ZnO films
   (1140-1155 photo)

10. No. 107 Vaidyanathan Subramanian

    In situ Growth and deposition of Quantum Dots onto Titania nanotubes via solvothermal method

# 國立交通大學博士班研究生

# 出席國際會議報告

| | | | |
|---|---|---|---|
| 報告人姓名 | 邱詩雅 | 報告日期 | 11/05/04 |
| 系所及年級 | 材料科學與工程學系（所）博士班二年級 | 核定文號 | 100 年 03 月 17 日<br>11D020 |
| 連絡電話 | 0932715907 | 電子信箱 | synthetic.mse96g@g2.nctu.edu.tw |
| 會議期間 | 11/05/01-06 | 會議地點 | 加拿大 蒙特婁 |
| 會議名稱 | （中文）第 219 屆美國電化學年會<br>（英文）219th Meeting of the Electrochemical Society | | |
| 發表論文題目 | （中文）使用高溫起孔洞劑合成介孔洞低介電材料及其孔洞型貌與電性之探討<br>（英文） Synthesis, Pore Morphology, and Dielectric Property of Mesoporous Low-k Material PSMSQ Using a Reactive High-Temperature Porogen, TEPSS | | |

報告內容包括下列各項：

一、 參加會議經過

二、 與會心得

三、 建議

四、 攜回資料名稱與內容

# 五、 其他

一、參加經過

本次第 219 屆美國電化學國際研討會（219th Meeting of the Electrochemical Society）之秋季會議於五月一日在加拿大「蒙特婁」盛大舉行，為期六日。在經過了二十幾個小時的飛行之後，學生抵達位於 Montreal Convention Center 大廳的會場報到，準備參加一連六天的研討會。此次學生之行程為：四月二十七日晚間十一點二十分由台灣桃園國際機場出發；五月十二日晚上九點三十分點返抵國門。

本會議為世界上最大型的電化學專業領域研討會之一，舉凡燃料電池、太陽能電池、電化學分析、、單層石墨應用半導體工業...等，都有非常多的熱門議題被討論，與會人士中不乏各領域產學界之國際知名專家。而學生的研究成果被安排在星期三（05/04）晚間 17:10 至 17:30 的 oral presentation，會議地點位於 Montreal Convention Center 的 Level 05 511 會議室。本次學生的發表方式為口頭簡報，過程中必須以英文與詢問者對答，過程緊張，但是事後相當有成就感，並獲得了畢生難忘的經驗。

二、心得（可含照片）

美國電化學國際研討會（秋季會議）為每年都會舉辦的大型科技會議之一，參加人數及論文數皆相當眾多，學術界與業界亦相當看重這個研討會，與會中很多論文議題內容相當充實，因此與其他參加者討論，都有相當收穫。因為報名人數眾多，為了避免有遺珠之憾，除了口頭成果報告之外，主辦大會還張貼各研究單位之研究成果海報，讓學生得以掌握國際上最新的研究動態。


圖片為會議中心一景。

圖片為與他校老師討論研究內容並交換心得。

圖片為此次會議所應邀的演講者。

圖片為大家聽演講的狀況。

此次學生所參加的場次為 E7 - Silicon Nitride, Silicon Dioxide, and Emerging Dielectrics，本場次有許多有關於新型低介電材料、、高介電材料、3D 內連接方式設計與可靠度的研究被發表，國際上各研究團隊更帶來許多精采的演講內容，令我大開眼界。另外，與會許多的專家學者對於學生所報告的題目給予了多寶貴的意見，讓學生獲益良多。

研究報告

a. Process challenges for integration of copper interconnects with Low-k dielectric
   Abst. # 1405
   可用 air gap 取代 low-k 材料，但仍有須考量的地方。

b. Pattern with amorphous carbon thin films
   Abst. # 1406
   Film density can be impacted by
   1. high temperature deposition (>500℃)
   2. ion bombardment during deposition

c. Ultra low dielectric constant materials for 22 nm technology node and beyond
   Abst. # 1407
   1. k < 2.0 需使用 air gap
   2. Light with wavelength > 200 nm is needed to preserve Si-$CH_3$ bonds.

3. Adjusting concentration avoid skeleton damage.

d. Development of porosimetry techniques for the characterization of plasma-treated porous ultra low-k materials

Abst. # 1408

1. Challenges of low-k: CMP, clean, sealing
2. 此研究提出使用 ＥＰ 可側 porosity
3. 此研究並利用ＳＰ 可測得 reflection index, pore size, and pore size distribution.

e. A new flexible quantum dot solar cell: heterostructural $TiO_2$ Mesh-$TiO_2$ nanoparticles photosensitized with CdS

Abst. # 106

1. SILAR process can be used for the formation of CdS nanocrystals on T_NT.
2. The addition of an intermediate $TiO_2$ layer through $TiCl_4$ treatment leads to increase in the deposition of CdS
3. The photoelectrochemical responses follow the order: T_NT/T_NP/CdS > T_NT/ CdS > T_NT

f. In situ grown and deposition of quantum dots onto Titania nanotubes via solvothermal method.

Abst. # 106

1. A solvothermal-based synthesis approach for deposition of high quality thick CdSe nanocrysral coating on T_NT has been demonstrated.
2. Exchanging myristate with thiolacetic acid followed by annealing in an inert atmosphere is highly beneficial.
3. The films demonstrate photoelectrochemical responses.

三、建議

很榮幸能有這個機會出國參加會議，站上國際會議的舞台發表自己的研究成果。當看見有人對自己的成果有興趣，或是和其他優秀學者互相討論，那種成就感真是難以言喻。也對於能夠了解全世界正在所在發展技術感到吃驚，認知到自己也該加緊腳步

而此次出國開會期間，其實最大的感受就是在於經費上的不足，補助款項（四萬多）僅可應付機票與部份報名費用，剩下報名費用及當地食宿實在無法應付。此趟旅程反而讓學生在經濟上有更大的負擔，希望國家能多補助這種相關會議的名額與金額，或是積極爭取頂尖會議於台灣舉辦，培養國內更多的優秀人才。

四、攜回資料名稱及內容

1. 本次會議行程（Meeting Program）
2. 論文發表時間表與論文摘要
3. 本次會議資料（隨身碟）
4. ECS 當期 Interface 雜誌

五、其他

無

# Synthesis, pore morphology, and dielectric property of mesoporous low-*k* material PSMSQ using a reactive high-temperature porogen, TEPSS

S.Y. Chiu, H.L. Hsu, M.L. Che, and J. Leu*
Department of Materials Science and Engineering,
National Chiao Tung University, Hsinchu, Taiwan
*1001 University Road, Hsinchu, Taiwan 30049
Tel: +886-3-5131420, Fax: +886-3-5724727,
E-mail: jimleu@mail.nctu.edu.tw

For porous low-*k* materials using a templating porogen, one of the challenges is the tendency of porogens to aggregate, leading to large pore size/distribution and exacerbated aggregation at higher porosity. Although reactive porogen is effective to limit porogen aggregation and reduce pore size [1], little work explores the reactive high-temperature porogen for the late-porogen removal integration scheme. In this study, a reactive high-temperature porogen, triethoxy-(polystyrene)silane (TEPSS) was synthesized by atom transfer radical polymerization (ATRP) [2] to obtain tight molecular weight (MW) distribution, then grafted onto the poly(methyl-silsesquioxane) (MSQ) matrix to circumvent the phase separation between matrix and porogen in the conventional hybrid approach. Upon the removal of polystyrene by thermal decomposition, uniformly distributed, spherical pores have been successfully achieved for mesoporous low-*k* MSQ films without porogen aggregation at high porosity up to 40% (k=2.37).

An extremely low polydispersity (1.06-1.12) of TEPSS was obtained by ATRP of styrene monomers with initiator, 3-chloropropyl(triethoxy)silane (CPTES) at 80 $^{o}$C for 12 hours, while MSQ precursor was obtained by sol-gel reaction of methyltrimethoxysilane (MTMS) in $HPF_6$ as schematically illustrated in Figs. 1(a) and (b). The high-temperature porogens, TEPSS at different loadings were then grafted onto MSQ matrix through sol-gel reaction at 50 $^{o}$C to yield porogen-grafted MSQ (PSMSQ) as shown in Fig. 1(c). The MW of TEPSS was investigated as a function of reaction solvents and the amount of initiator. Among three different solvents, molecular weight of TEPSS was 82,000 g/mole (dimethylformamide, DMF), 28,000 g/mole (toluene), and 26,000 g/mole (*p*-xylene), respectively. A lowest MW in *p*-xylene resulting from fast polymerization rate was due to the best match of solubility parameters between *p*-xylene (7.0) with CPTES (7.44) [3]. Meanwhile, high initiator content would also yield lower polymer molecular weight. The molecular weight was reduced from 26,000 g/mole to 3,500 g/mole when the ratio of CPTES/styrene was increased from 1/500 to 1/125. This could be attributed to the increased free radicals in the polymerization process with higher initiator content, leading to lower polymer MW [4]. The TEPSS with the lowest ($M_w$: 3,500 g/mole) in this study was obtained by using *p*-xylene at higher initiator concentration. The chemical structures and thermal properties of TEPSS porogen and PSMSQ low-k materials have been validated and examined by $^{1}$H-NMR, $^{29}$Si-NMR, FTIR, and TGA, which will be described in the full paper.

The porosity, pore morphology, and dielectric properties of PSMSQ porous low-*k* films using TEPSS ($M_w$: 3,500 g/mole) were then characterized by XRR, SEM, and C-V dot measurement. Porosity was found to increase from 16% to 54% while the dielectric constant was reduced from 2.66 to 2.18, when the porogen loading was increased from 0.4 to 43 wt%. The pore morphology of porous low-k MSQ films at various porosities are shown by SEM viewgraphs in Fig. 2: (a) 16%, (b) 27%, (c) 40%, and (d) 54%, respectively. At porosity ≤40%, the pores in the mesoporous films were found to be spherical and uniformly distributed. In addition, their pore size remained around 30 nm, indicating that little porogen aggregation occurred at porosity ≤40%. The obvious aggregation at porosity >40% will be further investigated and discussed.

Overall, this study introduced a novel method for preparing mesoporous materials, PSMSQ by using a reactive high-temperature porogen, TEPSS, suitable for the late-porogen removal integration scheme. In addition, the extremely low polydispersity by using ATRP and controllable reactivity of high-temperature porogen, TEPSS onto MSQ matrix yielded uniformly distributed and spherical pores (~30 nm) without aggregation at high porosity up to 40%.

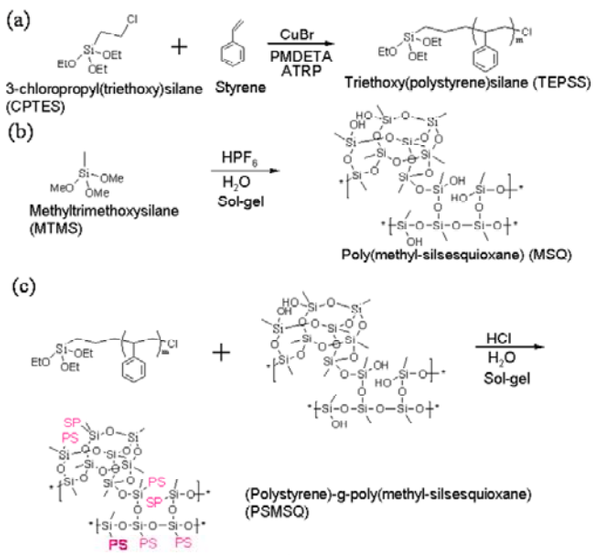


Fig. 1 Reaction schemes for (a) the high-temperature porogen, TEPSS, (b) MSQ matrix, and (c) porogen-grafted MSQ, PSMSQ

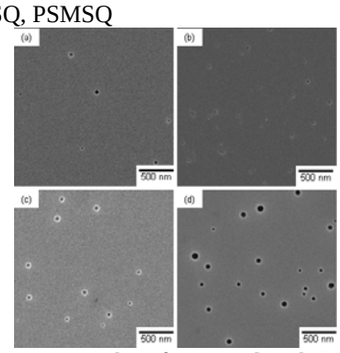


Fig. 2 SEM viewgraphs of porous low-k MSQ films at various porosities: (a) 16%, (b) 27%, (c) 40%, and (d) 54%

## References

[1] B. Lee, W. Oh, Y. Hwang, Y. H. Park, J. Yoon, K. S. Jin, K. Heo, J. Kim, K. W. Kim, and M. Ree, *Adv. Mater.*, **17**, 696 (2005)
[2] J. F. Lutz and K. Matyjaszewski, *Macromol. Chem. Phys.*, **203**, 1385 (2002)
[3] H. Chen, C. Wang, D. Liu, Y. Song, R. Qu, C. Sun, and C. Ji, *J Polym Sci Part A: Polym Chem*, **48**, 128 (2010)
[4] K. Matyjaszewski, J. L. Wang, T. Grimaud, and D. A. Shipp, *Macromolecules*, **31**, 1527 (1998)

# 國科會補助計畫衍生研發成果推廣資料表

日期:2011/09/30

| 國科會補助計畫 | 計畫名稱: 新穎接枝型起孔洞劑之多孔性低介電材料探討(I) |
|---|---|
| | 計畫主持人: 呂志鵬 |
| | 計畫編號: 99-2221-E-009-177- 學門領域: 固態電子 |

無研發成果推廣資料

# 99 年度專題研究計畫研究成果彙整表

| 計畫主持人：呂志鵬 | 計畫編號：99-2221-E-009-177- |
|---|---|
| 計畫名稱：新穎接枝型起孔洞劑之多孔性低介電材料探討(I) | |

| 成果項目 | | | 量化 | | | 單位 | 備註（質化說明：如數個計畫共同成果、成果列為該期刊之封面故事...等） |
|---|---|---|---|---|---|---|---|
| | | | 實際已達成數（被接受或已發表） | 預期總達成數(含實際已達成數) | 本計畫實際貢獻百分比 | | |
| 國內 | 論文著作 | 期刊論文 | 0 | 0 | 100% | 篇 | |
| | | 研究報告/技術報告 | 0 | 0 | 100% | | |
| | | 研討會論文 | 1 | 1 | 100% | | |
| | | 專書 | 0 | 0 | 100% | | |
| | 專利 | 申請中件數 | 0 | 0 | 100% | 件 | |
| | | 已獲得件數 | 0 | 0 | 100% | | |
| | 技術移轉 | 件數 | 0 | 0 | 100% | 件 | |
| | | 權利金 | 0 | 0 | 100% | 千元 | |
| | 參與計畫人力（本國籍） | 碩士生 | 0 | 0 | 100% | 人次 | |
| | | 博士生 | 0 | 0 | 100% | | |
| | | 博士後研究員 | 0 | 0 | 100% | | |
| | | 專任助理 | 0 | 0 | 100% | | |
| 國外 | 論文著作 | 期刊論文 | 0 | 1 | 100% | 篇 | 撰寫投稿至 JOURNAL OF THE ELECTROCHEMICAL SOCIETY 中 |
| | | 研究報告/技術報告 | 0 | 0 | 100% | | |
| | | 研討會論文 | 1 | 1 | 100% | | |
| | | 專書 | 0 | 0 | 100% | 章/本 | |
| | 專利 | 申請中件數 | 0 | 0 | 100% | 件 | |
| | | 已獲得件數 | 0 | 0 | 100% | | |
| | 技術移轉 | 件數 | 0 | 0 | 100% | 件 | |
| | | 權利金 | 0 | 0 | 100% | 千元 | |
| | 參與計畫人力（外國籍） | 碩士生 | 0 | 0 | 100% | 人次 | |
| | | 博士生 | 2 | 2 | 100% | | |
| | | 博士後研究員 | 0 | 0 | 100% | | |
| | | 專任助理 | 0 | 0 | 100% | | |

| | |
|---|---|
| 其他成果<br>(無法以量化表達之成果如辦理學術活動、獲得獎項、重要國際合作、研究成果國際影響力及其他協助產業技術發展之具體效益事項等，請以文字敘述填列。) | 無 |

| | 成果項目 | 量化 | 名稱或內容性質簡述 |
|---|---|---|---|
| 科教處計畫加填項目 | 測驗工具(含質性與量性) | 0 | |
| | 課程/模組 | 0 | |
| | 電腦及網路系統或工具 | 0 | |
| | 教材 | 0 | |
| | 舉辦之活動/競賽 | 0 | |
| | 研討會/工作坊 | 0 | |
| | 電子報、網站 | 0 | |
| | 計畫成果推廣之參與（閱聽）人數 | 0 | |

# 國科會補助專題研究計畫成果報告自評表

請就研究內容與原計畫相符程度、達成預期目標情況、研究成果之學術或應用價值（簡要敘述成果所代表之意義、價值、影響或進一步發展之可能性）、是否適合在學術期刊發表或申請專利、主要發現或其他有關價值等，作一綜合評估。

1. 請就研究內容與原計畫相符程度、達成預期目標情況作一綜合評估

■達成目標

□未達成目標（請說明，以 100 字為限）

□實驗失敗

□因故實驗中斷

□其他原因

說明：

2. 研究成果在學術期刊發表或申請專利等情形：

論文：□已發表 □未發表之文稿 ■撰寫中 □無

專利：□已獲得 □申請中 ■無

技轉：□已技轉 □洽談中 ■無

其他：(以 100 字為限)

3. 請依學術成就、技術創新、社會影響等方面，評估研究成果之學術或應用價值（簡要敘述成果所代表之意義、價值、影響或進一步發展之可能性）(以 500 字為限)

This proposal involves pioneering research on the preparation and synthesis of porous low-k materials through MSQ matrix grafted porogen (TEPSS-MSQ) approaches at low processing temperatures and the studies on the parameters and methods controlling the nano-/meso-pore size/distribution and their formation. In addition, this proposal will be the first attempt to our knowledge in developing a mesoporous structure with tight pore distribution through living radical polymerization, i.e. atom transfer radical polymerization (ATRP) to achieve very low polydispersity. The other contribution is our attempt to develop spin-on novel porous low-k films for as-deposited and late-porogen removal schemes through the grafting of novel functionalized high-temperature and low-temperature porogens (TEPSS and TEPMMAS) onto MSQ matrix. Moreover, we established the basic porogen properties such as decomposition temperature and thermal stability, the pore morphology and properties of porous low-k film in different porosity conditions. At the completion of this project, we expect to provide methodologies for designing ultra low-k materials ($k \leq 2.2$) with large porosity with small pore size and tight distribution for practical use for semiconductor industry such as the leading foundries TSMC and UMC in Taiwan.

The applications of such porous low-k materials are widespread； for example,

the TEPSS-MSQ or MSQ-g-PMMA porous low-k materials for (1) semiconductor applications in ILD layer, (2) diffuser in LCD-TFT, and others. The methodology can be applied to any porous materials required well-controlled pore size and pore distribution, in membranes for gas separation or fuel cell to name a few.